Enhancement of two-photon absorption in tetrapyrrolic compounds

Aliaksandr Karotki

Department of Physics, Montana State University, Bozeman, Montana 59717

Mikhail Drobizhev*

Lebedev Physics Institute, Leninsky Prospekt, 53, 119991 Moscow, Russia

Mikalai Kruk

Institute of Molecular and Atomic Physics, 70 F. Skaryna Avenue, 220072 Minsk, Belarus

Charles Spangler

Department of Chemistry and Biochemistry, Montana State University, Bozeman, Montana 59717

Erik Nickel

Synar Technologies, Inc., 1267 Briarwood Drive, Atlanta, Georgia 30306

Nugzar Mamardashvili

Institute of Solution Chemistry, Russian Academy of Sciences, Akademicheskaya St. 1, 153045 Ivanovo, Russia

Aleksander Rebane

Department of Physics, Montana State University, Bozeman, Montana 59717

We study the enhancement of two-photon absorption (TPA) in a series of porphyrins and tetraazaporphyrins by measuring the absolute TPA cross sections with 100-fs-duration pulses in two ranges of laser wavelengths, from 1100 to 1500 and from 700 to 800 nm. The cross section in the Q transition region is $\sigma_2 \sim 1$–10 GM (where 1 GM $= 10^{-50}$ cm^4 s^{-1} photons^{-1}), a value that is explained by partial lifting of the prohibition that is due to a parity selection rule. In the Soret transition region we find σ_2 enhancement by ~ 1 order of magnitude owing to the Q transition, which acts as a near-resonance intermediate state, and also owing to the presence of gerade energy levels, which we identify in this spectral region. In tetraazaporphyrins symmetrically substituted with strong electron acceptors, we find further enhancement (up to $\sigma_2 \sim 1600$ GM). As a possible application, we demonstrate for the first time to our knowledge the photosensitization of singlet-oxygen luminescence by TPA in porphyrin. © 2003 Optical Society of America

   OCIS codes: 190.4180, 190.4710, 300.6410.

1. INTRODUCTION

Two-photon absorption (TPA) is a third-order nonlinear-optical process in which two photons are absorbed simultaneously, such that the energy of the photons adds up to the energy of the excited atom or molecule, $h\nu_1 + h\nu_2 = E$.[1] In the past several years there has been increasing interest in this effect, especially because there is a variety of potential applications for TPA that ranges from frequency upconversion lasing[2] to photomedicine.[3] The fact that the rate of TPA is proportional to the square of the radiation intensity is used to increase the three-dimensional spatial selectivity of high-density optical data storage,[4,5] microfabrication,[4] and two-photon fluorescence microscopy.[6] Optical power limiting[7,8] takes ad-

vantage of the fact that low-intensity light propagates in TPA media practically without absorption, whereas high-intensity light is strongly attenuated.

   TPA in tetrapyrrolic molecules has potential applications for optical power limiting[8] and for holographic data storage.[5,9,10] Moreover, because tetrapyrrolic dyes serve as active structural units in various natural processes such as oxygen transport, photosynthesis, and electron transfer in cytochromes, they are uniquely suitable for various biomedical applications, including cancer treatment by photodynamic therapy.[3] So far, however, only a few measurements of TPA cross sections in tetrapyrrolic molecules have been reported in the literature. In particular, it was found that at $\lambda_{ex} = 1064$ nm

chlorophyll *a* shows $\sigma_2 = 8$ GM (Ref. 11; 1 GM $= 10^{-50}$ cm^4 s^{-1} photons^{-1}) and aluminum phthalocyanine shows $\sigma_2 = 12.7$ GM.[12] For protoporphyrin IX the following values were reported: $\sigma_2 = 0.7$ GM (λ_{ex} = 760 nm), $\sigma_2 = 0.9$ GM (λ_{ex} = 770 nm), $\sigma_2 = 0.6$ GM (λ_{ex} = 780 nm), and $\sigma_2 = 2.0$ GM (λ_{ex} = 790 nm).[13] The relative TPA spectra of several tetrapyrroles have been reported[14,15] but without absolute values of σ_2. Clearly, the TPA cross-section values given above are orders-of-magnitude too small for most of the applications mentioned above. Therefore, finding or creating new tetrapyrrolic compounds with higher values of σ_2 is of great practical importance.

To achieve the goal of our present study, i.e., to find ways to increase the TPA efficiency of tetrapyrrolic molecules, we use two main guidelines. First, several quantum-chemical calculations have predicted that in centrosymmetric porphyrins there may exist two-photon-allowed transitions that couple the *g*-parity ground state to an excited electronics state of the same parity (g–g transition).[16–24] The calculations place this strongly one-photon-forbidden transition near the one-photon-allowed Soret transition, which suggests that, if the laser frequency is tuned to 700–800 nm, the TPA cross section can undergo significant enhancement. In our experiments we study TPA in the Soret region with the specific goal of determining the g–g transition. Second, recent studies have shown that extension of the π-conjugation length and introduction of electron-donating (D) or electron-accepting (A) groups increases the TPA cross sections of linear π-conjugated molecules.[7,25] TPA cross-section values of as much as 4000 GM were obtained by Albota *et al.*,[25] who used linear D–A–D and A–D–A types of structures. Drobizhev *et al.*[26] used a D–π–D-type TPA chromophore as a repeat unit of three generations of dendrimers and obtained $\sigma_2 \sim 11{,}000$ GM, which is the highest so far of which we are aware for an organic molecule. Here we study correlations between the structure and the TPA properties in a series of tetrapyrrolic molecules and use them as guidelines to identify TPA-enhanced compounds.

We begin this paper by presenting a systematic measurement of the absolute TPA cross-section spectra of a series of free-base and zinc-substituted porphyrins and azaporphyrins. We study the TPA spectra in the laser wavelength region λ_{ex} = 1100–1400 nm, which corresponds to the transition from the ground state to the lowest excited singlet states and their vibronic satellites (*Q* bands). Then we study TPA at λ_{ex} = 700–800 nm, which corresponds to the Soret band region (B band). We discuss the nature of two-photon transitions in these two spectral regions, which we have found to be rather different. We show that in some porphyrins at λ_{ex} = 700–800 nm the TPA cross section is enhanced by almost 2 orders of magnitude. We explain this effect as being due to the influence of a nearby one-photon *Q* resonance and of two-photon-allowed g–g transitions, which we observe in the Soret band region. Next we study the influence of the electron-accepting substituents on the TPA cross section and show that its value can be further increased to $\sigma_2 = 1600$ GM. Finally, we use one of our new TPA-enhanced porphyrins to demonstrate the feasi-

bility of photosensitization of singlet molecular oxygen luminescence by near-IR illumination.

2. THEORETICAL CONSIDERATIONS

Consider two monochromatic laser beams, with frequencies ν_1 and ν_2, copropagating in an isotropic homogeneous molecular medium. None of the molecule's one-photon absorption frequencies coincides with ν_1 or ν_2. In this case the TPA cross section for a transition from the ground electronic state (0) to a final excited state (f) is given by the following expression for perturbation theory[21]:

$$\sigma_2 = \frac{(2\pi)^4 \nu_1 \nu_2}{(ch)^2} \frac{L^4}{n^2} \langle |S_{f0}|^2 \rangle g(\nu_1 + \nu_2), \qquad (1)$$

where n is the refractive index of the medium, $L = (n^2 + 2)/3$ is the Lorentz local field factor, and $g(\nu_1 + \nu_2)$ is the normalized line shape function [Hz^{-1}]. $\langle\ \rangle$ denotes the isotropic average over the molecular orientation. $|S_{f0}|^2$ represents the molecular two-photon tensor:

$$|S_{f0}|^2 = \left| \sum_i^N \left[\frac{(\hat{p}_1 \boldsymbol{\mu}_{i0})(\boldsymbol{\mu}_{fi}\hat{p}_2)}{\nu_{i0} - \nu_1 + i\Gamma_{i0}} + \frac{(\hat{p}_1 \boldsymbol{\mu}_{i0})(\boldsymbol{\mu}_{fi}\hat{p}_2)}{\nu_{i0} - \nu_2 + i\Gamma_{i0}} \right] \right|^2, \qquad (2)$$

where $\hat{p}_1$ and $\hat{p}_2$ are the unit polarization vectors of the two laser beams, ν_{i0} and Γ_{i0} are the frequency and the homogeneous linewidth associated with the ith state, respectively, $\boldsymbol{\mu}_{nm}$ is the transition dipole moment between states m and n ($m \neq n$) or the permanent dipole moment in state m ($m = n$). In our experiments both photons are derived from the same linearly polarized laser beam, such that $\hat{p}_1 = \hat{p}_2$ and $\nu_1 = \nu_2 = \nu_L$. In this case Eq. (2) simplifies to

$$|S_{f0}|^2 = \left| \sum_i^N \left[\frac{2(\hat{p} \boldsymbol{\mu}_{i0})(\boldsymbol{\mu}_{fi}\hat{p})}{\nu_{i0} - \nu_L + i\Gamma_{i0}} \right] \right|^2. \qquad (3)$$

One immediately can see that the magnitude of σ_2 increases if $|\boldsymbol{\mu}_{j0}|$ and $|\boldsymbol{\mu}_{fi}|$ increase and if the detuning of the excitation photon from intermediate levels, $\nu_{i0} - \nu_L$, decreases. Near resonance, if the detuning is small then the TPA process can be described to a good approximation by a three-level model, in which (apart from the ground and the final excited states) only one intermediate level is accounted for:

$$|S_{f0}|^2 = 4 \left| \frac{(\hat{p} \boldsymbol{\mu}_{i0})(\boldsymbol{\mu}_{fi}\hat{p})}{\nu_{i0} - \nu_L + i\Gamma_{i0}} + \frac{(\hat{p} \boldsymbol{\mu}_{00})(\boldsymbol{\mu}_{f0}\hat{p})}{\nu_{00} - \nu_L + i\Gamma_{00}} \right.$$
$$\left. + \frac{(\hat{p} \boldsymbol{\mu}_{f0})(\boldsymbol{\mu}_{ff}\hat{p})}{\nu_{f0} - \nu_L + i\Gamma_{f0}} \right|^2. \qquad (4)$$

The three terms on the right-hand side of Eq. (4) refer to the intermediate, the ground, and the final excited states, in that order. In this paper we study molecules that are either centrosymmetric or nearly centrosymmetric. A permanent dipole moment in this kind of porphyrin is typically below 0.5 Debye (D), whereas the transition dipole moment is of the order of 10 D. Therefore we can safely neglect the last two terms in Eq. (4).

The result of averaging over the molecular orientations depends on the angle between the dipole moment vectors, $\boldsymbol{\mu}_{i0}$ and $\boldsymbol{\mu}_{fi}$. For most of the molecules such data are not known. We assume that $\boldsymbol{\mu}_{i0}$ and $\boldsymbol{\mu}_{fi}$ are parallel, which gives following expression for the cross section:

$$\sigma_2 = \frac{4}{5} \frac{(2\pi)^4 \nu_L^2}{(ch)^2} \frac{L^4}{n^2} \frac{|\mu_{i0}|^2 |\mu_{fi}|^2}{(\nu_{i0} - \nu_L)^2 + \Gamma_{i0}^2} g(2\nu_L). \qquad (5)$$
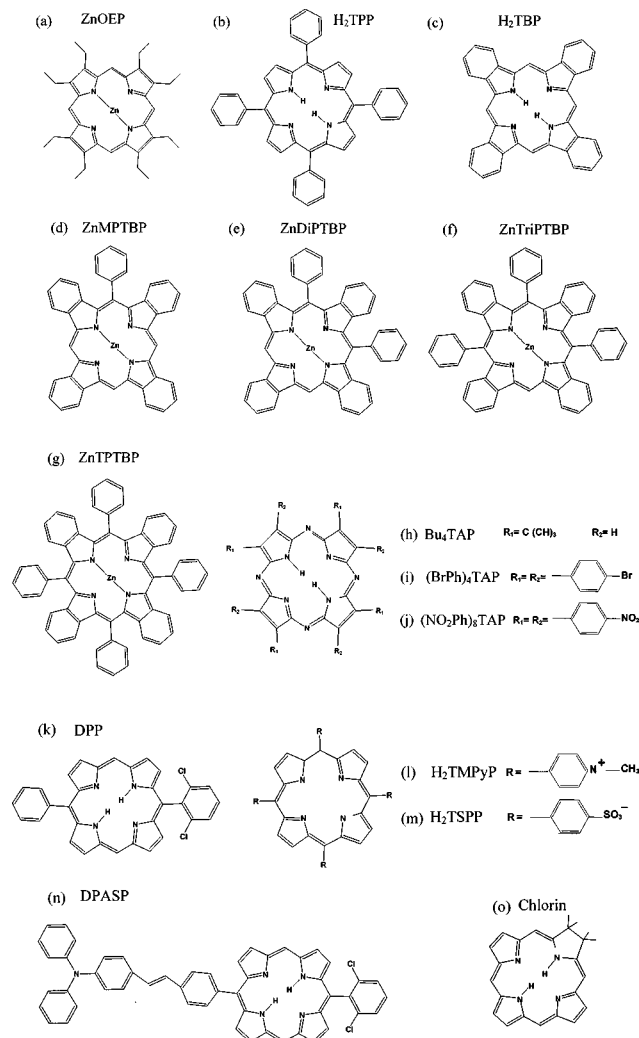

Fig. 1. Chemical structures of molecules discussed in this paper: (a) 2,3,7,8,12,13,17,18-octaethylporphine zinc (II) (ZnOEP); (b) 5,10,15,20-tetraphenylporphine (H$_2$TPP); (c) tetrabenzoporphine (H$_2$TBP); (d) 5-monophenyltetrabenzoporphine zinc (II) (ZnMPTBP); (e) 5,15-diphenyltetrabenzoporphine zinc (II) (ZnDiPTBP); (f) 5,10,15-triphenyltetrabenzoporphine zinc (II) (ZnTriPTBP); (g) 5,10,15,20-tetraphenyltetrabenzoporphine zinc (II) (ZnTPTBP); (h) 2,7,12,17-tetra-*tert*-butyl-tetraazaporphine (Bu$_4$TAP); (i) 2,3,7,8,12,13,17,18-(4-bromophenyl)-tetraazaporphine [(BrPh)$_8$TAP]; (j) 2,3,7,8,12,13,17,18-(4-nitrophenyl)-tetraazaporphine [(NO$_2$Ph)$_8$TAP]; (k) 5-phenyl,15-(2,6-dichlorophenyl)-porphine (DPP); (l) 5,10,15,20-tetrakis(4-*N*-methylpyridyl)-porphine (H$_2$TMPyP); (m) 5,10,15,20-tetrakis(4-sulfonatophenyl)-porphine (H$_2$TSPP); (n) 5-(4-diphenylaminostilbene), 15-(2,6-dichlorophenyl)-porphine (DPASP); (o) 7,8-dihydroporphine (chlorin).
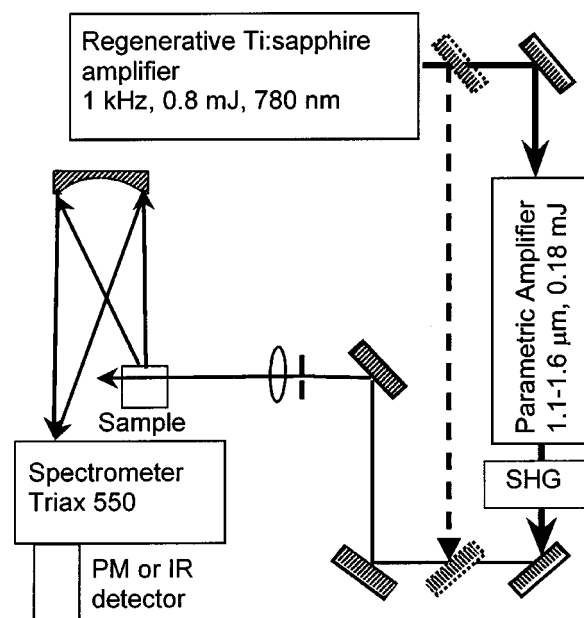

Fig. 2. Schematic of experimental setup: SHG, second-harmonic generator; PM, photomultiplier.

3. EXPERIMENT

Figure 1 shows the chemical structures of the compounds studied in this paper. We refer to them hereafter by their abbreviations given there: 2,3,7,8,12,13,17,18-octaethylporphine zinc (II) (ZnOEP), 5,10,15,20-tetraphenylporphine (H$_2$TPP), and 2,7,12,17-tetra-*tert*-butyl-tetraazaporphine (Bu$_4$TAP) were purchased from Aldrich. Tetrabenzoporphine (H$_2$TBP) was purchased from Porphyrin Products (Logan, Utah). 5-Monophenyl-tetrabenzoporphine zinc (II) (ZnMPTBP), 5,15-diphenyltetrabenzoporphine zinc (II) (ZnDiPTBP), 5,10,15-triphenyltetrabenzoporphine zinc (II) (ZnTriPTBP), and 5,10,15,20-tetraphenyltetrabenzoporphine Zinc (II) (ZnTPTBP) were synthesized and purified by A. M. Shul'ga.[27] 5-(4-Diphenylaminostilbene), 15-(2,6-dichlorophenyl)-porphine (DPASP), and 5-phenyl,15-(2,6-dichlorophenyl)-porphine (DPP) were synthesized and purified by E. Nickel. 2,3,7,8,12,13,17,18-(4-bromophenyl)-tetraazaporphine [(BrPh)$_8$TAP] and 2,3,7,8,12,13,17,18-(4-nitrophenyl)-tetraazaporphine [(NO$_2$Ph)$_8$TAP] were synthesized as reported in Refs. 28 and 29.

The laser system is shown in Fig. 2. It comprised a Ti:sapphire regenerative amplifier (CPA-1000 model, Clark-MXR, Inc.), which was operated at a 1-kHz repetition rate and produced 150-fs-long pulses (FWHM) of 0.8 mJ/pulse at $\lambda = 780$ nm. The pulses were parametrically down-converted in the optical parametric amplifier (TOPAS, Quantronix), which yielded 100-fs-long pulses (FWHM) in the range 1.1–1.6 μm with energy of 100–200 μJ per pulse. The laser spectrum was recorded with either a Perkin-Elmer Lambda 900 spectrophotometer coupled with a light-collecting fiber or with a Jobin Yvon/Spex TRIAX 550 spectrometer. The pulse duration and its temporal profile for both regenerative and optical parametric amplifiers were measured with an autocorrelator. Porphyrin fluorescence and singlet molecular-oxygen luminescence were collected and focused on the entrance

slit of the Jobin Yvon/Spex TRIAX 550 spectrometer with a spherical mirror and were measured, respectively, with photomultiplier and a liquid-nitrogen-cooled germanium IR detector.

To obtain the TPA spectra in the 700–820-nm wavelength region we frequency doubled the signal beam output of the optical parametric amplifier and focused the beam with an $f = 25$ cm lens onto the sample. The intensity of the visible fluorescence was detected as a function of the excitation wavelength, and the resultant spectra were scaled to an absolute value of σ_2 at 780 nm. We obtained that value by comparing the fluorescence intensities during two- and one-photon excitation, which were measured by use of the fundamental and the second-harmonic wavelengths, respectively, of the Ti:sapphire regenerative amplifier's output. A pinhole was placed immediately in front of the sample to ensure that the beam at the sample had the same radius for one- and two-photon excitation. Further details of the accompanying evaluation procedure are discussed in Appendix A. In the 1.1–1.4-μm wavelength region, both the absolute TPA cross section and the spectra were measured with the optical parametric amplifier. In the measurement of σ_2 we used either an $f = 50$ cm or an $f = 100$ cm focusing lens. The sample was placed off focus. In the experiment with singlet-oxygen generation we used the fundamental (average intensity, 15 W/cm^2) and the second-harmonic (average intensity, 0.5 W/cm^2) wavelengths of the Ti:sapphire amplifier. The laser beam was slightly focused to give a cylindrical volume of ~1.5-mm diameter in both cases.

We need to point out that the measured value of σ_2 is often strongly dependent on the duration of the laser pulses used in the experiment. If the pulse duration is comparable with the lifetime of the excited electronic state, which in organic molecules may reach several nanoseconds, the absorption may take place not only from the ground state but also from the excited state. As a result, the value of σ_2 obtained by use of nanosecond pulses often exceeds the true (instantaneous) cross section by several orders of magnitude.[30] In this respect, our current method based on two-photon-excited fluorescence with femtosecond pulses is well suited for measuring of the absolute TPA cross-section in our materials. Other methods based on nonlinear transmission usually require higher laser intensity and are often accompanied by competing nonlinear side effects such as stimulated emission, stimulated scattering, self-phase modulation, and continuum generation.[31]

4. RESULTS AND DISCUSSION

A. Two-Photon Absorption Spectra in the 1100–1400-nm Region

It is well known that if a molecule possesses a center of symmetry, then selection rules for one-photon and two-photon transitions are mutually exclusive: One-photon transitions occur between states with different parities ($g \rightarrow u$ or $u \rightarrow g$), whereas two-photon transitions are allowed between states with the same parity ($g \rightarrow g$ or $u \rightarrow u$). In our case, all molecules (except chlorin) possess a centrosymmetrical chemical structure (Fig. 1), and

one may expect the one- and two-photon spectra to be substantially different. Figure 3 shows the measured TPA cross sections of H$_2$TMPyP, H$_2$TSPP, H$_2$TPP, Bu$_4$TAP, (NO$_2$Ph)$_8$TAP, and chlorin in the laser wavelength region $\lambda_{ex} = 1100$–1400 nm. At the corresponding one-photon transition wavelengths ($\lambda_{tr} = 550$–700 nm) the linear absorption spectrum comprises four distinct bands, which are attributed, starting from the longest-wavelength band to the dipole-allowed vibrationless pure electronic transition $S_0 \rightarrow S_1$ $Q_x(0-0)$, its first vibronic satellite $Q_x(0-1)$, its second electronic transition $S_0 \rightarrow S_2$ $Q_y(0-0)$, and its
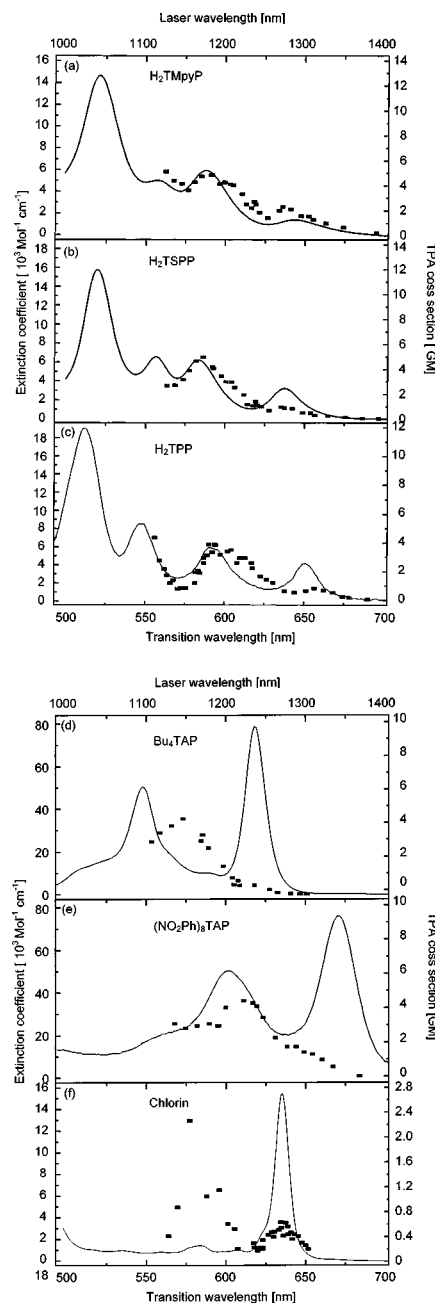

Fig. 3. TPA cross section as a function of transition wavelength in the Q region. Filled squares, TPA spectra; solid curves, linear absorption spectra; H$_2$TMPyP and H$_2$TSPP in water, H$_2$TPP in toluene, Bu$_4$TAP and (NO$_2$Bh)$_8$TAP in dichloromethane, and chlorin in poly(vinyl butyral) film.
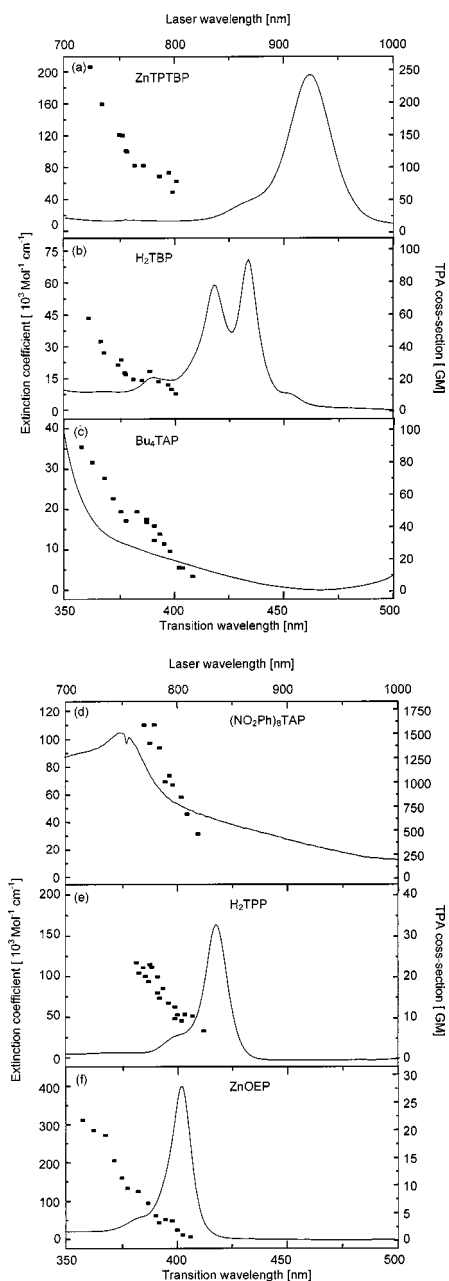
Fig. 4.   TPA cross section as a function of transition wavelength in the Soret region.   Filled squares, TPA spectra; solid curves, linear absorption spectra; ZnTPTBP and H_2TBP in toluene, H_2TBP in pyridine, and Bu_4TAP, $(NO_2Ph)_8TAP$, and ZnOEP in dichloromethane.

first vibronic satellite $Q_y(0-1)$.   Notice that the TPA spectra of porphyrins, i.e., H_2TMPyP, H_2TSPP, H_2TPP, and chlorin, resemble the characteristic structures in the respective linear absorptions.   In contrast, the tetraazaporphyrins Bu_4TAP and $(NO_2Ph)_8TAP$ show only the vibronic satellite, whereas the $Q(0-0)$ transition is missing.

To explain this behavior we note that all tetrapyrroles have a rich collection of vibrational modes of various degrees of symmetry in the frequency range $300-3000$ cm^{-1}, including noncentrosymmetrical vibrations.   It has been shown that the presence of such vibrations may lower a molecule's effective symmetry and make the TPA transi-

tion between the vibrationless ground electronic state and the vibronic excited states at least partially allowed.[32–34] The fact that different types of vibration contribute to one- and two-photon bands may explain the dissimilar shapes of the $Q_x(0-1)$ bands.   Vibrations should not, though, influence the pure electronic transition, and one still expects the TPA at the wavelength of the $Q_x(0-0)$ band to be minimal.   Both of our tetraazaporphyrins obey this rule quite well, which cannot be said of the non-aza-substituted porphyrins.   Accidental degeneracy between one- and two-photon transitions can be ruled out, first, because several different porphyrins show similar coincidence of TPA and $S_0 \rightarrow S_1$ transitions and, second, because theoretical calculations place the first parity-allowed transition at a much higher energy, near the Soret band.[16–24]   Another possible reason for eliminating accidental degeneracy may be that the TPA occurs either through electric quadrupole or magnetic dipole transitions.   However, both of these processes are less probable by a factor of $\sim 10^{-6}$ than the dipole-allowed TPA.   Inasmuch as our measured σ_2 is of the order of ~ 1 GM, these possibilities are excluded as well.   This result leads us to the conclusion that non-aza-substituted porphyrins are not entirely centrosymmetric.   The decrease in electronic symmetry may occur because of the presence of substituents and also because of the effects of solvents (or both). This conclusion is further strengthened by the fact that in chlorin, which is a distinctly noncentrosymmetric molecule, the 0–0 band is especially well pronounced in the TPA spectrum.   Also, the slightly broken symmetry of porphyrins can explain why the vibronic satellites tend to be stronger than the pure electronic band.   The absence of an exact center of symmetry permits weak TPA in both bands; however, coupling between electronic and vibronic levels significantly enhances the $Q_x(0-1)$ band.   In fact, by comparing the relative TPA intensities in $Q_x(0-1)$ and $Q_x(0-0)$ we can estimate to what degree the molecule's symmetry is preserved.   This information will be useful in the following discussion of $g-g$ transitions.

B.   Resonance Enhancement of Two-Photon Absorption in the Region of the Soret Transition
Figure 4 presents the TPA cross sections of ZnTPTBP, H_2TBP, Bu_4TAP, $(NO_2Ph)_8TAP$, H_2TPP, and ZnOEP in the region of the Soret transition.   Our data show that the characteristic value of σ_2 in the Soret region is considerably larger than that in the Q region.   For example, the maximum cross section of H_2TPP in the Soret region is ~ 25 GM, compared with 4 GM in the Q region.   In tetraazaporphyrins the increase is much more significant than in porphyrins.   In all cases the TPA increases monotonically toward shorter wavelengths.   In tetraazaporphyrins this behavior matches that of linear absorption, which also smoothly increases toward shorter wavelengths.   In non-aza-substituted porphyrins, however, the behavior of the TPA spectrum is completely different from that of linear absorption.

It is natural to explain the marked differences between TPA in the Soret and the Q regions by the fact that in the first case the energy of the photons comes rather close to the energy of the one-photon-allowed Q transitions, whereas in the second case there is no intermediate near-

resonance level. Indeed, we verified that for every experimental point presented in Figs. 3 and 4 the fluorescence intensity followed the quadratic dependence on the laser power. This is especially important for the short-wavelength data points in Fig. 4, for which we made sure that one-photon absorption that is due to the nearby $Q_x(0-0)$ band is insignificant. At even shorter wavelengths (not shown), the quadratic law gradually changed into a linear one.

To obtain a better qualitative picture of the resonance enhancement effect we have plotted the TPA data points as a function of the laser frequency (rather than of the transition wavelength), along with the one-photon absorption in the Q region. For ZnTPTBP, H$_2$TBP, and H$_2$TPP the laser frequency is rather close to the Q resonance. For tetraazaporphyrins and ZnOEP the detuning is larger, and association with the resonance is less obvious. To perform a quantitative analysis we turn to Eq. (5), which describes the TPA cross section as a function of the laser frequency detuning. By assuming that $g(2\nu_L)$ is constant (the validity of this assumption in the spectral region of interest is discussed below) and by differentiating Eq. (5) with respect to the laser frequency, we obtain the following relation between the normalized derivative of the TPA spectrum and the resonance frequency:

$$\alpha = \frac{1}{\sigma_{\text{TPA}}} \frac{d\sigma_{\text{TPA}}}{d\nu_L} = \frac{2}{\nu_L} + \frac{2(\nu_{i0} - \nu_L)}{(\nu_{i0} - \nu_L)^2 + \Gamma_{i0}^2}. \quad (6)$$

By rearranging Eq. (6) we can express the resonance frequency, ν_{i0}, as a function of measured parameters:

$$\nu_{i0} = \nu_L + \frac{\nu_L + [\nu_L^2 - \Gamma_{i0}^2(\nu_L\alpha - 2)^2]^{1/2}}{\nu_L\alpha - 2}. \quad (7)$$

The vertical arrows in Fig. 5 indicate an effective ν_{i0} calculated according to Eq. (7) based on the experimental data. We can use the deviation of the calculated frequency from the actual resonance frequency as a quantitative measure of the contribution of resonance enhancement to the TPA spectra. From an experimental point of view, this approach is reasonable because we have at our disposal only a relatively narrow section of the TPA spectrum, which would hardly permit a good fit to the full line shape function but is nevertheless sufficient for estimation of a derivative at a particular frequency. An advantage of this approach consists also in the need to use only relative values of TPA (one does not need absolute cross sections). Although the value of Γ_{i0} is known only approximately, we can take it to be equal to the homogeneous line width of the $Q_x(0, 0)$ band. In any case, if $\nu_{i0} - \nu_L \gg \Gamma_{i0}$, the result is not highly sensitive to the value of Γ_{i0}. For ZnTPTBP, H$_2$TBP, and Bu$_4$TAP we find good agreement between ν_{i0} and the actual $Q_x(0, 0)$ transition frequency. The fact that the actual resonance frequency is slightly lower is easily explained by the contribution from the $Q_x(0, 1)$ and other bands, which lie above the $Q_x(0, 0)$ band and which are not accounted for in the simple three-level model.

To further confirm the role of the $Q_x(0, 0)$ transition in resonance enhancement we compared the two-photon cross sections of several porphyrins, including a series of similar tetrabenzoporphyrins (ZnMPTBP, ZnDiPTBP,

ZnTriPTBP, and ZnTPTBP) at 780 nm (12 821 cm^{-1}). The linear absorption spectra of all these compounds are basically similar to that of ZnTPTBP; the only difference is that the strength of the $Q_x(0, 0)$ transition increases and shifts slightly to the red as the number of phenyl substituents increases. If we suppose that the TPA cross section at 780 nm is determined mainly by the resonance enhancement mechanism; then Eq. (5) predicts that σ_2 should be proportional to the square of the linear transition dipole moment $|\mu_{i0}|^2$ over the square of the frequency detuning, provided that $|\mu_{fi}|^2 g(2\nu_L) \sim \varepsilon_{fi}(2\nu_L - \nu_{i0})$ and does not vary much from one molecule to another. Indirect evidence that this last assumption is correct is
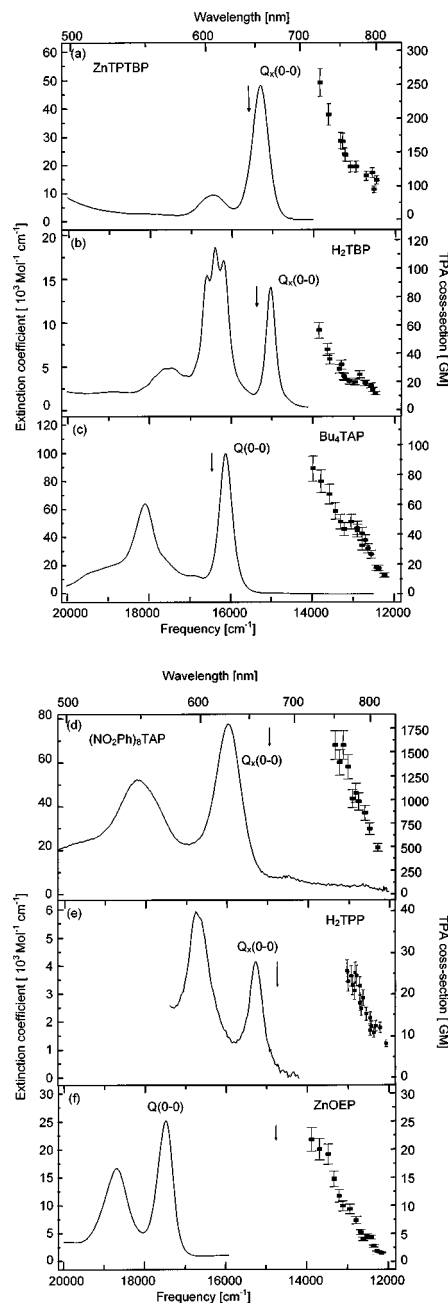

Fig. 5. TPA cross section as a function of excitation photon frequency (one half of the transition frequency) for the same molecules as in Fig. 4. Filled squares, TPA spectra; solid curves, linear absorption spectra.

Table 1. Summary of One- and Two-Photon Absorption Properties of Several Porphyrins

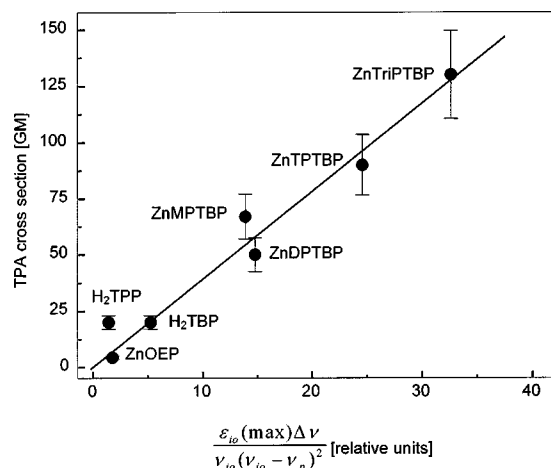| Porphyrin	Solvent	λ_{max} (nm)	$\bar{\nu}_{i0}$ (cm^{-1})	ε_{i0}(max) ($\times$mM^{-1} cm^{-1})	$\Delta\bar{\nu}$ (cm^{-1})	ε_{fi} (532 nm) ($\times$mM^{-1} cm^{-1})	σ_2 (GM)
H$_2$TPP	Toluene	647	15 500	3.4	470	15[35]	15
	Toluene					16[36]	
ZnTPP	CH$_2$Cl$_2$					16[35]	
	Toluene					18[36]	
H$_2$TBP	Pyridine	666	15 015	13	310		20
MgTBP	EP ^{a}					15[37]	
ZnMPTBP	Toluene	628	15 924	66	325		67
ZnDiPTBP	Toluene	632	15 810	56	370		50
ZnTriPTBP	Toluene	641	15 600	86	460		130
ZnTPTBP	Toluene	650	15 385	49	510		90
	Benzene					19[38]	

^{a}Diethyl ether/iso-propanol mixture (3/1,v/v).

Fig. 6. Correlation between the TPA cross section and a combination of linear absorption parameters for a number of porphyrins (see text for explanation).

found in picosecond transient absorption data. These data are collected in Table 1, which shows the literature values of singlet excited-state extinction, ε_{fi}, at λ_{fi} = 532 nm. It is evident that ε_{fi} (532 nm) does not vary by more than 25% on transition from a free-base tetraphenylporphin (TPP) to metallotetraphenylporphyrins (ZnTPP and MgTPP) and to tetrabenzo-substituted porphyrins (MgTBP and ZnTPTBP). Furthermore, it has been shown that for various porphyrins the transient singlet–singlet absorption spectra consist of a characteristic broad peak centered at approximately 440–510 nm, accompanied by a smooth tail in the region of 800–900 nm.[35] Whereas it is true that in our experiment we are probing a slightly different spectral region that corresponds to $\lambda_{fi} \sim$ 790–1100 nm, we can still assume that for all porphyrins in the current series the excited-state absorption will stay more-or-less the same.

Figure 6 shows the TPA cross sections of a number of similar porphyrins measured at 780 nm. If it is plotted as a function of the combination of linear absorption parameters, $\varepsilon_{i0}(\text{max})\Delta\bar{\nu}/[\bar{\nu}_{i0}(\bar{\nu}_{i0} - \bar{\nu}_L)^2]$, the dependence is well fitted to a straight line. This result substantiates our conclusion above that there is indeed a quantitative relation between σ_2 and the resonance enhancement factor, $|\boldsymbol{\mu}_{i0}|^2/(\nu_{i0} - \nu_L)^2$. However, this fact also supports

our conclusion about small variations in $|\boldsymbol{\mu}_{fi}|^2 g(2\nu_L)$ for the porphyrins studied. In this sense the behavior in a series of four phenyl-substituted tetrabenzoporphyrins is illustrative. As the number of the phenyl substituents increases from one to four, the lowest absorption band $Q_x(0-0)$ shifts to the red and its intensity increases, peaking for ZnTriPTBP, then slightly decreasing for ZnTPTBP. It is evident from Fig. 6 that both of these effects contribute to the resultant TPA cross section.

We can conclude that for the compounds shown in Fig. 6 (at least those with the highest σ_2 values), the enhancement of the TPA in the Soret region is indeed due primarily to the nearby intermediate $Q_x(0-0)$ transition. Furthermore, if the linear absorption from the ground state and that from the intermediate excited state are known, in this case the absolute value of σ_2 can be calculated directly from Eq. (5). For other molecules studied in this paper the intermediate Q resonance also contributes to the TPA value, but the resonance enhancement cannot be singled out as the predominant mechanism for TPA enhancement. For these other molecules we need to consider additional mechanisms that contribute to the enhancement in the Soret region.

C. Enhancement of Two-Photon Absorption Owing to $g-g$ Transitions

One can see from Fig. 6 that the value of ν_{i0} in $(\text{NO}_2\text{Ph})_8\text{TAP}$, H$_2$TPP, and ZnOEP is notably lower than the frequency of the $Q_x(0, 0)$ transition. Because the Q_x band is the lowest excited-singlet electronic state in porphyrins, this observation suggests that there is one or more energy levels in the Soret band region than those that are apparent from the linear absorption spectrum. We analyze this possibility in more detail by returning to the assumption made above that the function $g(2\nu_L)$ is constant. In Fig. 7 we plot the quantity $\sigma_2[(\nu_{i0} - \nu_L)^2 + \Gamma_{i0}^2]/\nu_L^2$ as a function of $2\nu_L$ for six different porphyrins. If the assumption above is correct, then, according to Eq. (5), this plot should yield a horizontal straight line. If the opposite is true, then this plot should give the effective spectrum of the line shape function, $g(2\nu_L)$. One can see that for ZnTPTBP and H$_2$TBP the dependence is nearly constant, which is in accord with our findings detailed in Subsection 4.B. For Bu$_4$TAP, the plot first in-

creases with frequency and then levels off into a broad and flat maximum. Note that in the calculation of ν_{i0} presented above we used only the nearly constant part of $g(2\nu_L)$. For the rest of the compounds, this plot shows a distinct dependence on frequency, which we can associate with a transition into a g-parity excited state. This assumption is supported by previous quantum-mechanical calculations carried out with different methods: the complete neglect of differential overlap/spectroscopic parameterization,[16–20] the self-consistent field molecular orbital formalism that uses π orbitals within the complete neglect of differential overlap formalism including full single and partial double configuration interaction,[21] *ab initio*,[22] and density functional theory,[23] which find a series of g-parity electronic energy levels, some of which lie
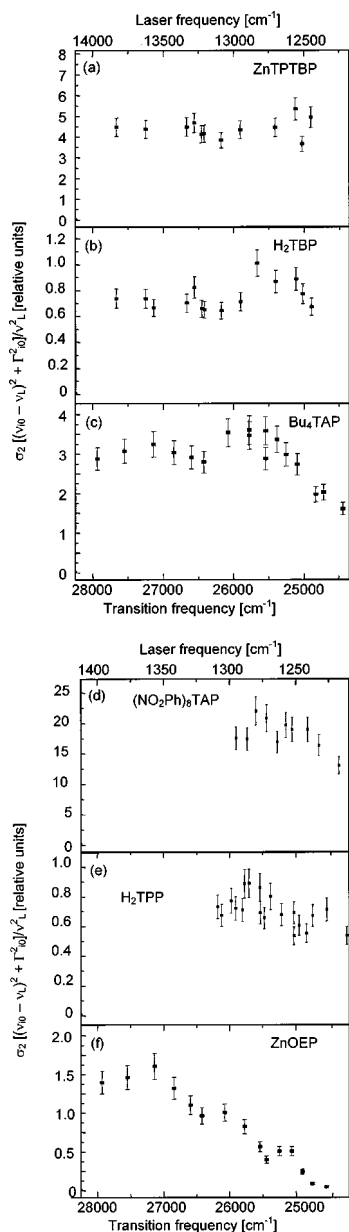

Fig. 7. Quantity $\sigma_2[(\nu_{i0} - \nu_L)^2 + \Gamma_{i0}^2]/\nu_L^2$ plotted as a function of $2\nu_L$ for the same molecules as in Fig. 4. A deviation from a straight horizontal line represents the spectral profile of the g–g transition.

in the spectral region considered here. In particular, for a number of free-base and metal-substituted porphyrins the lowest g-parity states are found to be near the Soret transition.[16–24] For free-base tetraazaporphin[19] (TAP) the calculations predicted that the first gerade level of A_g symmetry is at 25 500 cm^{-1}, and the next one, of B_{1g} symmetry, is at 26 500 cm^{-1}. Both of these calculated frequencies fall within the broad peak obtained in our experiments. Another calculation[24] gives 27 700 cm^{-1} for the first g–g transition in TAP, which is close to our experimental result. Dvornikov *et al.*[19] have suggested that the absence of a distinct Soret band in linear absorption of free-base TAP could be due to the overlap of many vibronic transitions into a g-parity $\pi\pi^*$ state.[19] For $(NO_2Ph)_8TAP$ we see approximately the same broad peak as for Bu$_4$TAP, and its maximum frequency (25 000–26 000 cm^{-1}) is in good agreement with the quantum-mechanical calculations[19,24] of TAP. We also note that theoretical calculations have predicted a large value, $\sigma_2 = 590$ GM, for free-base porphyrins.[21] This prediction corresponds well to our experimental observation that the TPA cross section in the Soret region is larger by an order of magnitude than that in the Q region, even if the resonance enhancement effect is ruled out.

Furthermore, experiments performed with time-resolved stepwise absorption in several porphyrins, including ZnTPTBP,[38] H$_2$TPP,[35] and ZnOEP,[35] have revealed that $S_1 \rightarrow S_n$ transitions into the Soret region show a smooth absorption tail, monotonically increasing toward higher energies. If we assume that the selection rules for stepwise absorption are the same as for simultaneous TPA, this absorption tail can be attributed to the overlap of several spectrally broad g–g transitions. We note that the $g(2\nu_L)$ spectrum of H$_2$TPP shown in Fig. 7(e) is in good agreement with the absorption spectra from the first singlet excited state obtained by Rodriguez *et al.*[35]

The considerations detailed above make our assignment of the structure observed in Fig. 6(c)–6(f) to the g–g transitions quite reasonable. The existence of the g–g transition explains also why for ZnOEP we still observe the dramatic tenfold increase of the value of σ_2 when we go from 12 225 to 14 000 cm^{-1}, even though any contribution from resonance enhancement is ruled out. For Bu$_4$TAP, $(NO_2Ph)_8TAP$, and H$_2$TPP we conclude that both the resonance enhancement effect and the g–g transition contribute nearly equally to the TPA spectrum.

D. Enhancement of TPA Two-Photon Absorption Owing to an Electron-Accepting Substitution

Figure 5(d) shows that the maximum σ_2 value of $(NO_2Ph)_8TAP$ amounts to 1600 GM at 12 990 cm^{-1} (770 nm). This constitutes, to our best knowledge, the highest intrinsic two-photon cross section ever reported for a tetrapyrrolic molecule. It has been noticed that attaching one or more chemical substituents with large electron-accepting ability increases the TPA cross sections of some organic molecules. Such a trend was noted previously for some stilbene derivatives with an A–D–A linear structure.[25] Theoretical considerations for linear quadrupolar centrosymmetrical molecules[39,40] and for three-branch octupolar molecules with C_3 symmetry[41] have
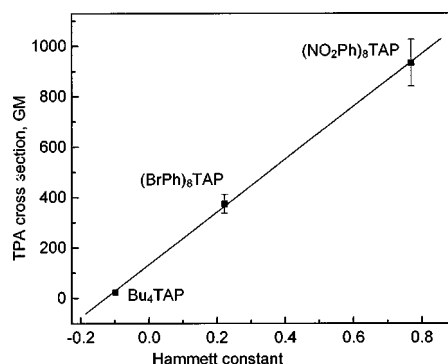
Fig. 8. Dependence of the TPA cross section (measured at the maximum $g–g$ transition) on the substituent's Hammett constant for three tetraazaporphyrins.

predicted that σ_2 will increase monotonically with the substituents' capability to accept or donate electrons. In particular, Lee *et al.*[41] predicted a linear correlation between the TPA cross section at the maximum of the $g–g$ transition and the Hammett constant (which characterizes the electron-accepting or -donating ability) of the substituent group.

Figure 8 shows the dependence of the TPA cross-section in the maximum $g–g$ transition on the substituent's Hammett constant[42] for three tetraazaporphyrin molecules, Bu_4TAP, $(BrPh)_8TAP$, and $(NO_2Ph)_8TAP$, and shows that σ_2 increases linearly with the acceptor strength. For example, from Bu_4TAP to $(NO_2Ph)_8TAP$ the cross section increases by ~37 times. From the linear absorption spectra we find that the corresponding change of $|\mu_{i0}|^2$ is ~1.5 times. At the same time, the resonance factor $1/[(\nu_{i0} - \nu_{fi})^2 + \Gamma_{if}^2]$ increases by a factor of 3. We conclude that the remaining eightfold increase is due to an increase of the symmetric charge-transfer contribution to the ground-state wave function.[40] The charge-transfer contribution manifests itself as increased coupling between the intermediate state and the final state, which in terms of Eq. (5) leads to a larger $|\mu_{fi}|^2$ value. Also, adding electron-accepting substituents may shift the intermediate energy level closer to resonance with the near-IR photons.[39–41,43] Our conclusion is that adding electron acceptors to the periphery of the tetrapyrrolic molecules increases all three factors denoted on the right-hand side of Eq. (5). We emphasize that p-NO_2 is one of the strongest known electron-acceptor groups. This means that with $(NO_2Ph)_8TAP$ we have likely reached the highest σ_2 value possible, at least for this type of porphyrin.

E. Two-Photon Excitation of Singlet Molecular-Oxygen Luminescence

Here we present one example of possible applications of enhanced TPA. The use of tetrapyrrolic molecules as photosensitizers for noninvasive treatment of tumors in photodynamic therapy[3] is well established and is based on the molecule's ability to generate cytotoxic singlet molecular oxygen. Because current photodynamic therapy requires illumination of the tumor area with visible light, the treatment of various cancers is limited by the small penetration depth of the visible light into strongly scattering and absorbing biological tissue. Two-photon photo-

sensitization was proposed to take advantage of the known fact that both absorption and scattering of light by tissues decrease at the so-called tissue transparency window, 750–1000 nm.[44] The main problem so far is that for commonly known porphyrins the TPA cross section typically does not exceed $\sigma_2 \sim 10$ GM.

Earlier in this paper we verified that the TPA cross section of some porphyrins can reach hundreds of GM (1 GM $= 10^{-50}$ cm^4 s^{-1} photons^{-1}) in the Soret band region. However, because the ability to generate singlet oxygen depends also on factors such as probability of intersystem crossing to the triplet state and the triplet-level lifetime, we found that the porphyrins studied so far are not suitable for this application. The successful approach turned out to be taking a standard porphyrin such as DPP [Fig. 1(k)] and attaching a diphenylaminostilbene chromophore in the meso position. The resultant diphenylaminostilbene porphyrin [DPASP, Fig. 1(n)] combines the high intersystem crossing rate and the long triplet lifetime of DPP with the large TPA cross section induced by the attached moiety. We note that earlier experiments with singlet-oxygen generation by TPA used exclusively nontetrapyrrolic photosensitizers,[45] which makes our approach much more relevant for photodynamic therapy.

Figure 9 shows the TPA spectra of two porphyrins, DPP and DPASP, near the Soret band. Although both compounds exhibit a distinctive $g–g$ transition band, the maximum cross section of the modified porphyrin DPASP is almost an order of magnitude larger than that of the parent molecule. Figure 10(a) shows a near-IR luminescence spectrum obtained on one-photon (dashed curve) and two-photon (solid curve) excitation of a solution of DPASP in toluene. The characteristic peak at 1276 nm identifies this spectrum with singlet molecular-oxygen luminescence. Furthermore, if nitrogen gas were bubbled through the solution, the intensity of the peak would decrease because of the decreased oxygen concentration.
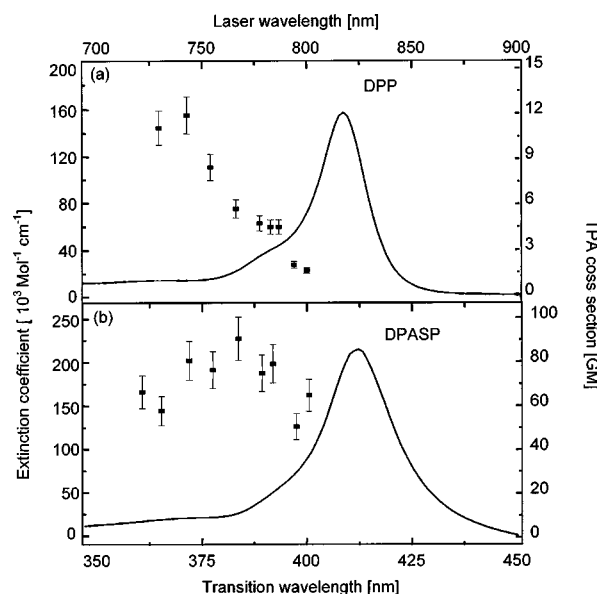

Fig. 9. TPA cross section as a function of transition wavelength in the Soret region. Filled squares, TPA spectrum; solid curves, linear absorption. DPP and DPASP in toluene.
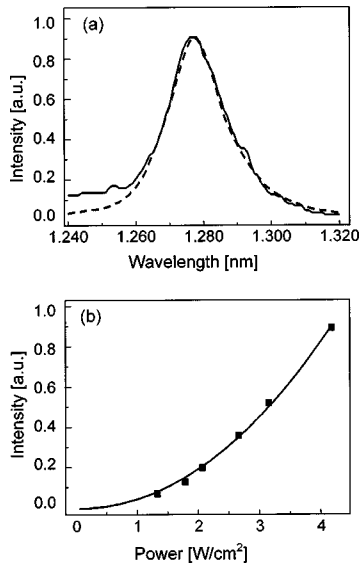
Fig. 10. (a) $^1\Delta_g \rightarrow {}^3\Sigma_g^-$ luminescence spectra of molecular oxygen in an air-saturated toluene solution of DPASP. Dashed curve, one-photon excitation; solid curve, two-photon excitation. Both spectra are normalized to unity. (b) Dependence of $^1\Delta_g \rightarrow {}^3\Sigma_g^-$ oxygen luminescence intensity I_Δ on average illumination intensity P on two-photon excitation. Filled squares, experimental data; solid curve, best power-law fit, $I_\Delta = aP^n$ with $n = 2.1 \pm 0.1$.

Figure 10(b) shows the measured luminescence peak intensity at 1276 nm plotted as a function of laser intensity. The quadratic dependence verifies that the singlet-oxygen luminescence signal is indeed generated by TPA. In a äseparate experiment we were able to detect singlet-oxygen luminescence on two-photon excitation of the water-soluble porphyrin H_2TMPyP. We note that this porphyrin forms complexes with proteins and with DNA,[46,47] which makes our result especially relevant in the context of photodynamic therapy.

5. CONCLUSIONS

We have described experiments in which we measured the absolute cross section of two-photon absorption (TPA) in an extended family of porphyrins and tetraazaporphyrins by using 100-fs-duration pulses in two ranges of wavelengths, 700–800 and 1100–1500 nm. We analyzed TPA spectra by using a three-level model and showed that in the Q-band region the characteristic cross section, $\sigma_2 \sim 1$–10 GM, is due to partial breaking of ungerade symmetry of the excited electronic state. We showed that the symmetry breaking is less in tetraazaporphyrins than in non-aza-substituted porphyrins. We determined that in the Soret region TPA efficiency is enhanced by an order of magnitude as a result of a near-resonant Q transition. We used a three-level description effectively to separate out the contributions to TPA from resonance enhancement and have reported, for the first time to our knowledge, the spectral contours of gerade symmetry energy levels. We achieved a further substantial enhancement of TPA, to $\sigma_2 \sim 1600$ GM, by introducing symmetrical electron-accepting substitutions in tetraazaporphyrin and showed that σ_2 increases in proportion to the substitu-

ent's Hammett constant. We have also demonstrated for what we believe is the first time photosensitization of singlet-oxygen luminescence by TPA in porphyrins.

APPENDIX A: EVALUATION OF THE ABSOLUTE TPA CROSS SECTION

Consider a homogeneous two-photon absorbing medium of length L and molecular density n irradiated by a laser pulse of intensity $I_0(r, t)$, where r is the distance from the geometrical center of the pulse to the observation point and t is the time. The intensity just after the sample will be

$$I(r, t) = \frac{I_0(r, t)}{1 + \sigma_2 n L I_0(r, t)} \tag{A1}$$

If the absorption is weak, i.e., if $\sigma_2 n L I_0(r, t) \ll 1$, then

$$I(r, t) \simeq I_0(r, t)[1 - \sigma_2 n L I_0(r, t)]. \tag{A2}$$

The total energy absorbed from the pulse can be found by integration over the pulse duration and the volume of the sample:

$$\Delta E_{\text{TPA}} = \sigma_2 n L \int_0^\infty 2\pi r \mathrm{d}r \int_{-\infty}^\infty \mathrm{d}t I_0^2(r, t). \tag{A3}$$

In our experiment we used a pinhole of radius $r_0 < r_L$ in front of the sample (r_L is the radius of the laser beam), and to a good approximation we can neglect variation of the intensity within r. In the time domain the pulse intensity had a nearly Gaussian shape:

$$I_0(r, t) = I_{0i} \exp\left(-\frac{4t^2 \ln 2}{\tau^2} \right), \tag{A4}$$

where I_{0i} is the pulse intensity at its maximum and τ is a time duration of the pulse (FWHM):

$$\Delta E_{\text{TPA}} = \frac{\sigma_2 n L \pi^{3/2} r_0^2 I_{0i}^2 \tau}{\sqrt{8 \ln 2}}. \tag{A5}$$

If we substitute the peak intensity of the pulse through its total energy,

$$E_{i\text{TPA}} = \int_0^{r_0} 2\pi r \mathrm{d}r \int_{-\infty}^\infty \mathrm{d}t I_{0i} \exp\left(-\frac{4t^2 \ln 2}{\tau^2} \right)$$

$$= \frac{\pi^{3/2} \tau r_0^2 I_{0i}}{2\sqrt{\ln 2}}, \tag{A6}$$

then we obtain the following expression for the absorbed energy:

$$\Delta E_{\text{TPA}} = \frac{\sqrt{2 \ln 2}\, \sigma_2 n L E_{i\text{TPA}}^2}{\pi^{3/2} \tau r_0^2}. \tag{A7}$$

The number of excited molecules in the sample is

$$N_{\text{TPA}} = \frac{\Delta E_{\text{TPA}}}{2h\nu_{2\text{ph}}} = \frac{\sqrt{2 \ln 2}\, \sigma_2 n L E_{i\text{TPA}}^2}{2h\nu_{2\text{ph}} \pi^{3/2} \tau r_0^2}, \tag{A8}$$

where h is the Planck constant and $\nu_{2\text{ph}}$ is the frequency of the two-photon excitation light.

For one-photon excitation, the energy absorbed by the same sample is

$$\Delta E_{1\text{PA}} = E_{i1\text{PA}}[1 - \exp(-\sigma_1 n L)] \simeq E_{i1\text{PA}} \sigma_1 n L, \tag{A9}$$

where E_{i1PA} is the energy of laser pulse and σ_1 is the one-photon (linear) absorption cross section. The number of excited molecules is

$$N_{1PA} = \frac{\Delta E_{1PA}}{h\nu_{1ph}} = \frac{\sigma_1 n L E_{i1PA}}{h\nu_{1ph}}, \qquad (A10)$$

where ν_{1ph} is the frequency of the one-photon excitation. If TPA and one-photon excitation share the same geometry, then the corresponding fluorescence intensities, F_{TPA} and F_{1PA}, should be proportional to the number of excited molecules in each case. We also suppose that quantum yield of the fluorescence does not depend on the mode of excitation. The ratio of the fluorescence intensities is

$$\frac{F_{TPA}}{F_{1PA}} = \frac{\sqrt{2\ln 2}\,\sigma_2 E_{iTPA}^2 \nu_{1ph}}{2\nu_{2ph}\pi^{3/2}\tau r_0^2 \sigma_1 E_{1PA}}, \qquad (A11a)$$

which leads to the final expression for the TPA cross section:

$$\sigma_2 = \frac{F_{TPA}\nu_{2ph}\sqrt{2}\,\pi^{3/2}\tau r_0^2 E_{1PA}}{F_{1PA}\nu_{1ph}\sqrt{\ln 2}\,E_{iTPA}^2}\,\sigma_1. \qquad (A11b)$$

A. Rebane's e-mail address is rebane @physics.montana.edu.

*Permanent address: Department of Physics, Montana State University, Bozeman, Montana 59717.

REFERENCES

1. M. Göppert-Meyer, "Elementartakte mit zwei Quantensprüngen," Ann. Phys. (Leipzig) **9**, 275–294 (1931).
2. G. S. He, P. P. Markowicz, T.-C. Lin, and P. N. Prasad, "Observation of stimulated emission by direct three-photon excitation," Nature **415**, 767–770 (2002).
3. B. W. Henderson and T. J. Dougherty, "How does photodynamic therapy work?" Photochem. Photobiol. **55**, 147–157 (1992).
4. B. H. Cumpston, S. P. Ananthavel, S. Barlow, D. L. Dyer, J. E. Ehrlich, L. L. Erskine, A. A. Heikal, S. M. Kuebler, I.-Y. S. Lee, D. McCord-Maughon, J. Qin, H. Röckel, M. Rumi, X.-L. Wu, S. R. Marder, and J. W. Perry, "Two-photon polymerization initiators for three-dimensional optical data storage and microfabrication," Nature **398**, 51–54 (1999).
5. M. Drobizhev, A. Karotki, and A. Rebane, "Persistent spectral hole burning by simultaneous two-photon absorption," Chem. Phys. Lett. **334**, 76–82 (2001).
6. W. Denk, J. H. Strickler, and W. W. Webb, "Two-photon laser scanning fluorescence microscopy," Science **248**, 73–76 (1990).
7. C. W. Spangler, "Recent developments in the design of organic materials for optical power limiting," J. Mater. Chem. **9**, 2013–2020 (1999).
8. G. L. Wood, M. J. Miller, and A. G. Mott, "Investigation of tetrabenzoporphyrin by the Z-scan technique," Opt. Lett. **20**, 973–975 (1995).
9. A. Rebane, R. Kaarli, P. Saari, A. Anijalg, and K. Timpmann, "Photochemical time-domain holography of weak picosecond pulses," Opt. Commun. **47**, 173–176 (1983).
10. M. Drobizhev, C. Sigel, and A. Rebane, "Phototautomer of Br-porphyrin: a new frequency-selective material for ultrafast time–space holographic storage," J. Lumin. **86**, 391–397 (2000).
11. N. N. Vsevolodov, L. P. Kostikov, L. P. Kayushin, and V. I. Gorbatenkov, "Two-photon absorption of laser radiation by

chlorophyll a and some organic dyes," Biophysics (USSR) **18**, 755–757 (1973).
12. Yu. P. Meshalkin, E. E. Alfimov, N. E. Vasil'ev, A. N. Denisov, V. K. Makukha, and A. P. Ogirenko, "Two-photon excitation of aluminum phthalocyanines," Quantum Electron. **29**, 1066–1068 (1999).
13. R. L. Goyan and D. T. Gramb, "Near-infrared two-photon excitation of protoporphyrin IX: photodynamics and photoproduct generation," Photochem. Photobiol. **72**, 821–827 (2000).
14. E. A. Wachter, W. P. Partridge, W. E. G. Fisher, H. C. Dees, and M. G. Petersen, "Simultaneous two-photon excitation of photodynamic therapy agents," in *Commercial Applications of Ultrafast Lasers*, M. K. Reed, ed., Proc. SPIE **3269**, 68–75 (1998).
15. I. Suzuka, M. Kozawa, and Y. Numata, "Two-photon absorption spectra of porphyrins—first observation of the hidden *g*-excited state," presented at the XVIII International Union of Pure and Applied Chemistry Symposium on Photochemistry, Dresden, Germany, July 19–22, 2000.
16. V. A. Kuzmitsky and K. N. Solovyov, "Calculation of electronic spectra of porphin molecule by PPDP/S method," J. Appl. Spectrosc. **27**, 724–730 (1977).
17. V. I. Gael', V. A. Kuzmitsky, and K. N. Solovyov, "All-valence calculation by fragments of electronic spectrum of Mg-tetraphenylporphyrin molecule," J. Appl. Spectrosc. **63**, 790–798 (1996).
18. V. A. Kuz'mitskii, "Excited even-symmetry states of metallocomplexes of porphin and its derivatives," J. Appl. Spectrosc. **68**, 758–765 (2001).
19. S. S. Dvornikov, V. N. Knyukshto, V. A. Kuzmitsky, A. M. Shulga, and K. N. Solovyov, "Spectral-luminescent and quantum-chemical study of azaroporphyrin molecules," J. Lumin. **23**, 373–392 (1981).
20. V. G. Maslov, "Calculations of electronic spectra of Mg–P, Mg–Pc and their ionic forms by the PPDP/S method," Theor. Exp. Chem. (USSR) **20**, 288–298 (1984).
21. M. B. Masthay, L. A. Findsen, B. M. Pierce, D. F. Bocian, J. S. Lindsey, and R. R. Birge, "A theoretical investigation of the one- and two-photon properties of porphyrins," J. Chem. Phys. **84**, 3901–3915 (1986).
22. H. Nakatsuji, J. Hasegawa, and M. Hado, "Excited and ionized states of free base porphin studied by symmetry adapted cluster-configuration interaction (SAC-CI) method," J. Chem. Phys. **104**, 2321–2329 (1996).
23. D. Sundholm, "Density functional theory study of the electronic absorption spectrum of Mg-porphyrin and Mg-etioporphyrin," Chem. Phys. Lett. **317**, 392–399 (2000).
24. E. Orti, M. C. Piqueras, R. Crespo, and J. L. Bredas, "Influence of annelation on the electronic-properties of phthalocyanine macrocycles," Chem. Mater. **2**, 110–116 (1990).
25. M. Albota, D. Beljonne, J.-L. Brédas, J. E. Ehrlich, J.-Y. Fu, A. A. Heikal, S. E. Hess, T. Kogej, M. D. Levin, S. R. Marder, D. McCord-Maughon, J. W. Perry, H. Röckel, M. Rumi, G. Subramaniam, W. W. Webb, X.-L. Wu, and C. Xu, "Design of organic molecules with large two-photon absorption cross sections," Science **281**, 1653–1656 (1998).
26. M. Drobizhev, A. Karotki, and A. Rebane, "Dendrimer molecules with record large two-photon absorption cross section," Opt. Lett. **26**, 1081–1083 (2001).
27. A. M. Shul'ga, senior staff researcher, Institute of Molecular and Atomic Physics of National Academy of Sciences, 70 F. Skaryna Avenue, 220072 Minsk, Belarus.
28. N. V. Chizhova and V. D. Berezin, "Nitration of octaphenyl-meso-tetraazaporphine," Zh. Org. Khim. **30**, 1678–1680 (1994).
29. N. V. Chizhova, O. G. Khelevina, and V. D. Berezin, "Bromation of porphyrins," Izv. Vyssh. Uch. Zav. Khim. Khim. Tekh. **37**, 20–23 (1994).
30. G. P. Das, R. Vaia, A. T. Yeates, and D. S. Dudis, "A theoretical model for excited state absorption," Synth. Metals **116**, 281–283 (2001).
31. D. A. Oulianov, I. V. Tomov, A. S. Dvornikov, and P. M. Rentzepis, "Observations on the measurement of two-photon absorption cross-section," Opt. Commun. **191**, 235–243 (2001).
32. M. W. Dowley, K. B. Eisenthal, and W. L. Peticolas, "Two-

photon laser excitation of polycyclic aromatic molecules," J. Chem. Phys. **47**, 1609–1619 (1967).

33. B. Honig and J. Jortner, "Theoretical studies of two-photon absorption processes. I. Molecular benzene," J. Chem. Phys. **46**, 2714–2727 (1967).

34. V. I. Bredikhin, M. D. Galanin, and V. N. Genkin, "Two-photon absorption and spectroscopy," Sov. Phys. Usp. **16**, 299–321 (1973).

35. J. Rodriguez, C. Kirmaier, and D. Holten, "Optical properties of metalloporphyrin excited states," J. Am. Chem. Soc. **111**, 6500–6506 (1989).

36. W. Blau, H. Byrne, W. M. Dennis, and J. M. Kelly, "Reverse saturable absorption in tetraphenylporphyrins," Opt. Commun. **56**, 25–29 (1985).

37. H. Stiel, A. Volkmer, I. Rückmann, A. Zeug, B. Ehrenberg, and B. Röder, "Non-linear and transient absorption spectroscopy of magnesium(II)-tetrabenzoporphyrin in solution," Opt. Commun. **155**, 135–143 (1998).

38. P. Chen, I. V. Tomov, A. S. Dvornikov, M. Nakashima, J. F. Roach, D. M. Alabran, and P. M. Rentzepis, "Picosecond kinetics and reverse saturable absorption of meso-substituted tetrabenzoporphyrins," J. Phys. Chem. **100**, 17,507–17,512 (1996).

39. W.-H. Lee, M. Cho, S.-J. Jeon, and B. R. Cho, "Two-photon absorption and second hyperpolarizability of the linear quadrupolar molecule," J. Phys. Chem. A **104**, 11,033–11,040 (2000).

40. M. Barzoukas and M. Blanchard-Desce, "Molecular engineering of push–pull dipolar and quadrupolar molecules for two-photon absorption: a multivalence-bond states approach," J. Chem. Phys. **113**, 3951–3959 (2000).

41. W.-H. Lee, H. Lee, J.-A. Kim, J.-H. Choi, M. Cho, S.-J. Jeon, and B. R. Cho, "Two photon absorption and nonlinear optical properties of octupolar molecules," J. Am. Chem. Soc. **123**, 10,658–10,667 (2001).

42. D. H. McDaniel and H. C. Brown, "An extended table of Hammett substituent constants based on the ionization of substituted benzoic acids," J. Org. Chem. **23**, 420–427 (1958).

43. E. Zojer, D. Beljonne, T. Kogej, H. Vogel, S. R. Marder, J. W. Perry, and J.-L. Bredas, "Tuning of two-photon absorption response of quadrupolar organic molecules," J. Chem. Phys. **116**, 3646–3658 (2002).

44. S. Wan, J. A. Parrish, R. R. Anderson, and M. Madden, "Transmittance of nonionizing radiation in human tissues," Photochem. Photobiol. **34**, 679–681 (1981).

45. P. K. Frederiksen, M. Jørgensen, and P. R. Ogilby, "Two-photon photosensitized production of singlet oxygen," J. Am. Chem. Soc. **123**, 1215–1221 (2001).

46. N. N. Kruk, S. I. Shishporenok, A. A. Korotky, V. A. Galievsky, V. S. Chirvony, and P.-Y. Turpin, "Binding of the cationic 5,10,15,20-tetrakis(4-*N*-methylpyridyl) porphyrin bound at 5′CG3′ and 5′GC3′ sequences of hexadeoxyribonucleotides: triplet–triplet transient absorption, steady-state and time-resolved fluorescence and resonance Raman studies," J. Photochem. Photobiol., B **45**, 67–74 (1998).

47. B. M. Dzhagarov, M. M. Kruk, V. S. Chirvony, V. A. Galievsky, and P.-Y. Turpin, "Guest–host complexes of porphyrins with DNA: porphyrin excited states deactivation channels and interaction with molecular oxygen," *Advances in Porphyrin Chemistry*, O. Golubchikov, ed. (St. Petersburg University Publishing House, St. Petersburg, Russia, 1999), pp. 50–69.